MNRAS **000**, 1–14 (0000) Preprint 26 February 2016 Compiled using MNRAS LATEX style file v3.0

Modelling nova populations in galaxies

Hai-Liang Chen[1,2,3,4⋆], T. E. Woods[1,5], L. R. Yungelson[6], M. Gilfanov[1,7,8], Zhanwen Han[2,3]
[1] *Max Planck Institute for Astrophysics, Karl-Schwarzschild-Str. 1, Garching b. München 85741, Germany*
[2] *Yunnan Observatories, Chinese Academy of Sciences, Kunming, 650011, China*
[3] *Key Laboratory for the Structure and Evolution of Celestial Objects, Chinese Academy of Sciences, Kunming 650011, China*
[4] *University of Chinese Academy of Sciences, Beijing 100049, China*
[5] *Monash Centre for Astrophysics, 19 Rainforest Walk, Monash University, VIC, 3800, Australia*
[6] *Institute of astronomy, RAS, 48 Pyatnitskaya Str., 119017 Moscow, Russia*
[7] *Space Research Institute of Russian Academy of Sciences, Profsoyuznaya 84/32,117997 Moscow, Russia*
[8] *Kazan Federal University, Kremlevskaya str.18, 420008 Kazan, Russia*

arXiv:1602.07849v1 [astro-ph.SR] 25 Feb 2016

Accepted XXX. Received YYY; in original form ZZZ

ABSTRACT

Theoretical modelling of the evolution of classical and recurrent novae plays an important role in studies of binary evolution, nucleosynthesis and accretion physics. However, from a theoretical perspective the observed statistical properties of novae remain poorly understood. In this paper, we have produced model populations of novae using a hybrid binary population synthesis approach for differing star formation histories (SFHs): a starburst case (elliptical-like galaxies), a constant star formation rate case (spiral-like galaxies) and a composite case (in line with the inferred SFH for M31). We found that the nova rate at 10 Gyr in an elliptical-like galaxy is $\sim 10-20$ times smaller than a spiral-like galaxy with the same mass. The majority of novae in elliptical-like galaxies at the present epoch are characterized by low mass white dwarfs (WDs), long decay times, relatively faint absolute magnitudes and long recurrence periods. In contrast, the majority of novae in spiral-like galaxies at 10 Gyr have massive WDs, short decay times, are relatively bright and have short recurrence periods. The mass loss time distribution for novae in our M31-like galaxy is in agreement with observational data for Andromeda. However, it is possible that we underestimate the number of bright novae in our model. This may arise in part due to the present uncertainties in the appropriate bolometric correction for novae.

Key words: binaries: close — novae, cataclysmic variables — white dwarfs, galaxies: individual: M31

1 INTRODUCTION

As a subclass of accreting white dwarfs, novae are important objects for the study of binary evolution and nucleosynthesis (see Patterson 1984; Gehrz et al. 1998, for a review). Given that WDs undergoing nova eruptions may gain mass during accretion, it has been suggested that they may be the progenitors of type Ia supernovae in some variants of the single degenerate scenario (e.g. Starrfield et al. 1988; Yungelson et al. 1996; Hachisu & Kato 2001). Novae are believed to be important sources of some nuclides, such as ^{7}Li, ^{15}N, ^{17}O, ^{22}Na and ^{26}Al (e.g. Starrfield et al. 1978; Hernanz et al. 1996; Gehrz et al. 1998; Kudryashov et al. 2000) which in some cases have been actually observed (Tajitsu et al. 2015; Izzo et al. 2015; Tajitsu et al. 2016). Although novae have been widely studied, many questions remain unclear. In recent years, an increasing number of observational studies of novae have become available. It is vital to compare our present theoretical understanding with observations, in particular the properties of nova populations on the whole.

It is accepted that novae occur in an accreting WD binary with accretion rates below the stable burning regime, whereby the H-rich material burns unstably on the surface of the WD (e.g. Mestel 1952a,b; Kraft 1964; Giannone & Weigert 1967; Tutukov & Yungel'Son 1972; Paczynski & Zytkow 1978; Sion et al. 1979; Tutukov & Ergma 1979). But note, **Idan et al. (2013)** found that in the high accretion rate regime which is conventionally considered as corresponding to 'stable' H-burning, the latter actually proceeds in small-scale short-timescale flashes. In order to understand the process underlying nova explosions, considerable effort has been made in producing simulations of nova

⋆ E-mail: chenhl@ynao.ac.cn

© 0000 The Authors

explosions (e.g. Starrfield et al. 1972; Prialnik et al. 1978, 1979; Sion et al. 1979; Prialnik & Kovetz 1995; Yaron et al. 2005). During the accretion phase, first, H-rich material will be accumulated on the surface of the WD and gradually compressed by more accreted material. The H-rich shell will be heated by the compression and undergo a thermonuclear runaway (TNR), when the pressure at the bottom of the accreted envelope becomes sufficiently high and the degeneracy is lifted. The TNR will lead to ejection of the accreted mass. If the accretion rate is close to the stable burning regime, the nova explosion is relatively weak and only a fraction of the accreted mass will be ejected. If the accretion rate is low enough, nova explosions are strong and the WD will be eroded. Prialnik & Kovetz (1995) and Yaron et al. (2005) have simulated a large number of multicycle nova evolution models. They found that the properties of novae (e.g. ignition mass, maximum luminosity) are mainly determined by the WD mass, accretion rate and the interior temperature. They show different characteristics of novae for accreting WDs with different parameters within the possible ranges. Based on the results of these simulations, many general properties of individual nova can be understood.

In the past three decades, observations of novae in different Hubble types of galaxies have been undertaken (e.g. Ciardullo et al. 1990; Della Valle et al. 1994; Shafter et al. 2000; Ferrarese et al. 2003; Williams & Shafter 2004; Coelho et al. 2008; Franck et al. 2012). These observations are very helpful to study nova properties in different stellar populations. Previous studies (e.g. Duerbeck 1990; Della Valle et al. 1992) suggested that there are two kinds of nova population: the disk novae and bulge novae. The disk novae are fast and may harbour more massive WDs, compared with the bulge novae (Della Valle & Livio 1998). Some observational studies (e.g. Ciardullo et al. 1990; Shafter et al. 2000; Ferrarese et al. 2003; Williams & Shafter 2004) have suggested that luminosity-specific nova rates may not evolve strongly with the Hubble type of galaxies and the average luminosity-specific nova rate is around $2\times10^{-10}\,{L_{\rm K,\odot}}^{-1}\,{\rm yr}^{-1}$. However, several studies indicate that some galaxies, such as the Magellanic Clouds, M33 and others, may have higher luminosity-specific nova rates (e.g. Della Valle et al. 1994; Della Valle 2002; Neill & Shara 2005; Alis & Saygac 2014; Shara et al. 2016).

Regarding individual galaxies, novae in M31 have been intensively studied in the past (e.g Arp 1956; Rosino 1964, 1973; Ciardullo et al. 1987; Rosino et al. 1989; Shafter & Irby 2001; Darnley et al. 2006). Some earlier results suggested a nova rate in M31 of $\sim 20-40$ ${\rm yr}^{-1}$ (see Shafter & Irby (2001) and their table 1). Darnley et al. (2006) performed a careful analysis of the distribution and the incompleteness of novae in their survey, and derived a nova rate of $65^{+16}_{-15}\,{\rm yr}^{-1}$. These studies have also provided other key parameters in describing nova properties (e.g. decay time, peak magnitude), which can be directly compared with theoretical results.

With the binary population synthesis method, Yungelson et al. (1997) found that the luminosity-specific nova rate should be significantly higher in younger stellar populations compared with older stellar populations. The typical WD mass of novae in young stellar populations is larger than in old stellar populations. In addition, Nelson et al. (2004) modelled the Galactic nova population (assuming a constant SFR and 100% initial binarity) and found that their derived nova rate and orbital period distribution are in agreement with observations.

In this paper, with a hybrid binary population synthesis method, we model the nova population for galaxies with two representative star formation histories (SFHs), i.e. starburst and constant star formation rate (SFR). Moreover, in order to compare with nova surveys of M31, we have computed a composite model with a star formation history consistent with that which is presently inferred for M31 (see Robertson et al. 2004, and discussion below). We will present our predicted nova rates, as well as the characteristic distribution of novae for different models, such as the WD mass, peak magnitude, mass loss time, and compare these results with observations.

The paper is structured as follows. In section 2, we introduce our binary population synthesis approach and describe how we calculate the values of various nova properties in our simulation models. In section 3, we mainly show the results of these simulations and compare these results with observations. We have a further discussion in section 4, before summarizing our results in section 5.

2 BINARY POPULATION SYNTHESIS

In this paper, we adopt a hybrid binary population synthesis approach, which was first introduced in Chen et al. (2014). In this approach, first, we use the BSE code (Hurley et al. 2002) to generate WD binaries with non-degenerate donors (i.e. main sequence (MS), Hertzsprung gap (HG), red giant (RG) stars). Then we follow the evolution of these WD binaries with a grid of detailed evolutionary tracks computed with MESA code (Paxton et al. 2011, 2013). Compared with other binary population synthesis approaches, this method allows a careful treatment of the second mass transfer phase. Here we briefly summarize the main assumptions and ingredients in our calculation.

2.1 BSE calculation

We adopt the initial mass function (IMF) of Kroupa (2001) for the primary mass ranging from $0.1\,{\rm M}_\odot$ to $100\,{\rm M}_\odot$. We take a flat mass ratio distribution (Kraicheva et al. 1979) and a flat distribution in logarithmic space for binary separations in the range between 10 and $10^6{\rm R}_\odot$. With respect to the binary fraction, observations indicate that it may depend on the binary parameters (Kouwenhoven et al. 2009; Kraus & Hillenbrand 2009; Sana et al. 2012). Following the suggestion of van Haaften et al. (2013), we adopt the following formula for the binary fraction ($f_{\rm b}$):

$$f_{\rm b} = 0.50 + 0.25{\rm log}_{10}(M_1), \quad (1)$$

where M_1 is the primary mass. This is different from our previous papers (Chen et al. 2014, 2015), in which we adopt a constant binary fraction, i.e. 50%. However, this does not significantly influence our results.

With the BSE population synthesis code (Hurley et al. 2002), we computed the evolution of around 2×10^6 binary systems, a fraction of which may evolve into a binary system consisting of a WD and a non-degenerate donor that later stably overflows Roche lobe. We follow the evolution of these systems until the WD binaries become semi-detached and

obtain the binary parameters (i.e. WD mass, donor mass, orbital period) at the onset of mass transfer.

It is worth noting that we include different types of donors (i.e. MS, HG, RG donors) in our calculation. In previous studies of nova populations (e.g. Nelson et al. 2004), only MS donors are included. However, Darnley et al. (2014) have shown that some recurrent novae harbour HG and RG donors, though some of these may reside in symbiotic binaries. Therefore, for the first time, we include a relatively complete set of progenitors of novae binaries in a population synthesis study.

2.2 Binary evolution calculation

In order to follow the evolution of these WD binaries, we computed the evolution of a grid of WD binaries with varying initial parameters using the detailed stellar evolutionary code MESA (Paxton et al. 2011, 2013). In this grid, the WD mass ranges from $0.50\,\mathrm{M}_\odot$ to $1.35\,\mathrm{M}_\odot$ with a step $\Delta M = 0.10\,\mathrm{M}_\odot$. We ignore He WDs in our calculation.[1] The donor mass ranges from $0.10\,\mathrm{M}_\odot$ to $13.5\,\mathrm{M}_\odot$ with a step $\Delta M = 0.05\,\mathrm{M}_\odot$. The orbital period ranges (with step size $\Delta\log_{10}P_{\rm orb} = 0.1$) from 1000 days down to the minimum period for which the binary separation yields mass transfer which begins on the zero-age main sequence. With the binary parameters at the onset of mass transfer from our BSE calculations, we can select the closest track in the grid of MESA calculation and follow the evolution of any WD binaries.

In the MESA calculation, we adopt the limits for the stable burning regime from Wolf et al. (2013). We assume that the excess mass will be lost in the form of an optically thick wind (Hachisu et al. 1996) and take away the specific angular momentum of the WD, if the accretion rate is larger than the maximum stably burning rate. If the accretion rate is in the stably burning regime, we assume that no mass will be lost. If the accretion rate is below the stable burning regime, we adopt the H burning retention efficiency from Yaron et al. (2005), as approximated in Chen et al. (2014) (see their Eq. 6). Regarding the He burning retention efficiency, this suffers from considerable uncertainties (e.g. Hachisu et al. 1999; Kato & Hachisu 2004; Piersanti et al. 2014; Hillman et al. 2015). Here we simply use the prescription from Hachisu et al. (1999). The angular momentum lost due to mass loss during nova explosion is rather uncertain (see e.g. Livio et al. 1991; Nelemans et al. 2016; Schreiber et al. 2016). Here we assume that the lost mass takes away the specific angular momentum of the WDs.

In our calculation, we adopt an initial hydrogen abundance $X = 0.70$, helium abundance $Y = 0.28$ and metallicity $Z = 0.02$.

2.3 Calculation of the nova rate

In our calculations, we do not compute the detailed evolution of the WDs. We consider the WD as a point mass and compute its mass evolution. From our binary evolution calculations, for any given WD binary evolutionary track, we know the accretion rate and WD mass. Yaron et al. (2005) computed multicycle nova models for WDs under differing conditions, and showed the dependence of nova properties on WD mass, accretion rate and WD temperature (see their tables 2 and 3). Under certain assumptions on the interior temperature of the WDs, we can then find the characteristics of Novae, such as the ignition and ejected mass, by interpolating their tables. The results of Townsley & Bildsten (2004) indicate that, for WD masses and accretion rates typical of cataclysmic variables, equilibrium WD core temperatures are smaller than 1.0×10^7 K. However, there is no complete computation similar to Yaron et al. (2005) for different WDs with low temperatures. Therefore, we use $T_{\rm c} = 1.0 \times 10^7$ K in our calculations. In section 4, we will discuss its influence on our results.

2.4 Common envelope evolution

For the treatment of common envelope (CE) events, we adopt the α-formalism (Webbink 1984; de Kool 1990) and use the fitting formula from Loveridge et al. (2011) for the binding energy parameter λ. The efficiency α suffers from considerable uncertainty (see Ivanova et al. 2013, for a review). Davis et al. (2012) found that the value of α should be ≤ 1.0 and it may decrease with increasing WD mass and secondary mass. By reconstructing the evolution of post CE binaries, Zorotovic et al. (2010) constrain the value of α to be in the range of $0.2-0.3$. A similar result is found by Ricker & Taam (2012) using hydrodynamic simulations. Davis et al. (2010) found that a global value of $\alpha > 0.10$ provides a good agreement with observations of post CE binaries. Therefore, in our calculation, we adopted $\alpha = 0.25$. We will discuss the influence of this value on our results in section 4.

By default, we adopt criteria for dynamically stable mass loss from Hjellming & Webbink (1987) and Webbink (1988) (hereafter the HW criteria) for binaries with giant stars. However, some detailed binary evolution calculations (e.g. Han et al. 2002; Chen & Han 2008) indicate that this criteria may predict too low a critical mass ratio, and that the critical mass ratio should depend on the evolutionary phase of the donor star, mass, and adapted mode of angular momentum loss from the system. Woods & Ivanova (2011) (see also Passy et al. 2012) demonstrated that the difference is due to consideration of the superadiabatic outer surface layer, whose typical thermal timescale may be smaller than the timescale for mass transfer. The muted response of this surface layer of the donor in response to mass loss (relative to mass loss directly from the convective envelope, as in polytropic models), allows for stable mass transfer at higher mass ratios than previously considered. Recently, Pavlovskii & Ivanova (2015) found that the critical mass ratio may vary from 1.5 to 2.2.

2.5 Binary population synthesis models

With the uncertainties in the treatment of CE events in mind, we computed three different models: a025 model, a025qc15 model, a025qc17 model. In all of these models, we use $\alpha = 0.25$. In the first model, we use the HW criteria for

[1] Nelson et al. (2004) computed the nova rates from He WDs by extrapolating the results of Prialnik & Kovetz (1995) and found that He WDs contribute a very small fraction ($\lesssim 5\%$) to the total nova rates.

giant stars. In the other models, we use critical mass ratios $q_c = 1.5$ and 1.7 for giant stars, respectively. However, we should emphasize that the critical ratio should not be a fixed value and varies as a function of other stellar parameters, as mentioned above.

In each model, we consider three different SFHs, which may roughly represent three kinds of galaxies. (I) Elliptical-like galaxies: all stars (with initial total mass $10^{11}\,M_\odot$) are formed at $t = 0$. (II) Spiral-like galaxies: a constant SFR for 10 Gyr with total stellar mass $10^{11}\,M_\odot$ formed. (III) M31-like galaxies: In order to compare wtih observations of novae in M31, we make a composite model with a SFH outlined as follows. Robertson et al. (2004) simulated the formation and SFH of disk galaxies, which Olsen et al. (2006) have demonstrated to be consistent with the observationally derived SFH of M31. Given that the total stellar mass of M31 is around $1.1 \times 10^{11}\,M_\odot$ (Barmby et al. 2007), we adopt the SFH from Robertson et al. (2004) as the SFH of M31 and rescale the total stellar mass to $1.1\times10^{11}\,M_\odot$. In this model, the SFR increases from $t = 0$ Gyr and peaks around $t = 2.0$ Gyr, and then declines by around one order of magnitude by 10 Gyr.

3 RESULTS

3.1 Evolution of nova population with stellar ages

In Fig. 1, we show the evolution of nova rates for elliptical-like and spiral-like galaxies in different models. The mass-normalized nova rates reach maximum around 1 Gyr in elliptical-like galaxies and around 2 Gyr in spiral-like galaxies. After the maximum, it declines by ∼2 orders of magnitude in elliptical-like galaxies and by a factor of ∼4 in spiral-like galaxies by the age of 10 Gyr. A similar behaviour in elliptical galaxies is also found in Matteucci et al. (2003). In elliptical-like galaxies, at ∼1 Gyr, the typical donor mass of WD binaries is around $2\,M_\odot$. For these binaries, WDs will efficiently accumulate mass during a thermal timescale mass transfer. These massive WDs have frequent outbursts. With increasing stellar age, the typical donor mass will decrease. The WD can not efficiently accumulate mass and the typical WD mass decreases. Therefore, the nova rate will decrease. In spiral-like galaxies, novae form with a typical delay time around 1 Gyr. Therefore, after ∼2 Gyr, the nova rate is almost constant while the stellar mass continues to increase linearly with time. Therefore, the mass-specific nova rates at old ages in the right panel of Fig. 1 decrease as t^{-1}.

Compared with our a025 model, the nova rates in a025qc15 and a025qc17 are smaller. In a025qc15 and a025qc17 models, the critical mass ratios for a CE in binaries with giant stars are larger than when using the HW criteria. Therefore, it will become more difficult for binaries to enter a CE and fewer accreting WD binaries will be produced. Consequently, the nova rates decrease as this critical mass ratio increases.

The nova rates at 10 Gyr in different models for different kinds of galaxies are shown in table 1. For an elliptical-like galaxy with $10^{11}\,M_\odot$, the nova rate is around $10 - 20\,\mathrm{yr}^{-1}$. For a spiral-like galaxy with the same mass, the nova rate is around 10-20 times larger. These results are in line with Matteucci et al. (2003) who found that the luminosity-specific nova rates in elliptical galaxies are lower than in spiral and irregular galaxies. Yungelson et al. (1997) came to a similar conclusion using a binary population synthesis method. In M31-like galaxies, the nova rate is around $80 - 160\,\mathrm{yr}^{-1}$. Darnley et al. (2006) detected 20 classical novae in M31 and deduced a global nova rate of $65^{+16}_{-15}\,\mathrm{yr}^{-1}$ based on a thorough analysis of the completeness of novae in their survey. However, as they discussed, the novae with the shortest decay times t_2 or t_3 (the decline time of the optical light curve from the peak by 2 (3) magnitudes) in their sample are likely incomplete because of insufficient cadence of the survey. In order to get a reliable nova rate for M31, Soraisam & Gilfanov (2015) and Soraisam et al. (2016) combined the data from observations of novae with $t_2 < 20$ days by Arp (1956) with the data of novae with $t_2 > 20$ days from Darnley et al. (2006), taking the completeness into consideration. In the incompleteness analysis of Arp's survey, they ran Monte-Carlo simulations and used a template nova light curve and an observed maximum magnitude-rate of decline relation. Then they can get the fraction of detected novae as a function of t_2 (see Appendix of Soraisam et al. (2016) for more details). Regarding the incompleteness of Darnley's survey, we use a completeness value of ≈ 23% for correction based on the result of Darnley et al. (2006) (see their table 3). The nova rate is computed as follows.

$$\dot{N}(t_2) = \begin{cases} \frac{N}{\eta\times1.342\times6.02\times10^{10}}, & \text{for Arp's data} \\ \frac{N}{\eta\times2.830\times(0.47\times11\times10^{10})}, & \text{for Darnley's data.} \end{cases}$$

where $\dot{N}(t_2)$ is in unit of $\mathrm{yr}^{-1}\ M_\odot{}^{-1}$, N is the observed numbers of sources at t_2 and η is the completeness. The duration of the two surveys are 1.342 yr and 2.830 yr respectively. The masses enclosed by the field of view in the two surveys are $6.02\times10^{10}\,M_\odot$ and $5.17\times10^{10}\,M_\odot$, respectively (see Soraisam et al. (2016) for more details). Then we obtain a global nova rate $97\,\mathrm{yr}^{-1}$ [2] for M31. Our results are in good agreement with this number. In order to make a further comparison, we compare the distributions of predicted and observed mass loss time distribution of novae in the following section.

In order to understand the evolution of nova populations with time, in Fig. 2, we show the isodensity contours of nova parameters at different stellar ages for elliptical-like galaxies in our a025 model. Using Yaron et al. (2005) data we can find the maximum luminosity of novae and then convert it to M_v (see the following section). From these plots, it is found that the average WD mass of a nova population decreases with increasing stellar ages, which is consistent with previous studies, e.g. Politano (1996). According to the results of Yaron et al. (2005), the mass loss times and recurrence periods of novae with massive WDs are shorter compared with novae with smaller WD mass (see also Truran & Livio 1986; Politano et al. 1990). Therefore, it is expected that the typical mass loss time and recurrence time of populations of novae will increase with increasing stellar age. Similarly, the typical maximum magnitude of novae become lager as the stellar age increases.

[2] In Soraisam et al. (2016), they found a nova rate of 106 yr^{-1}, corresponding to the $\theta = 1.0$ case of Darnley et al. (2006). Here, we use the $\theta = 0.18$ case of Darnley et al. (2006). θ is the ratio of nova rates per unit r' flux of the disc and bulge population.

Table 1. The current nova rates (i.e. at 10 Gyr) for different kinds of galaxies in different models. The total stellar mass for elliptical-like and spiral-like galaxies is 10^{11} $M_\odot$ and it is 1.1×10^{11} $M_\odot$ for M31-like galaxies. The present nova rate of M31 galaxy is around 97 yr^{-1} (see text).

model	α	q_c	WD temperature (T_c) (10^7 K)	nova rate (yr^{-1}) (elliptical-like)	nova rate (yr^{-1}) (spiral-like)	nova rate (yr^{-1}) (M31-like)
(1)	(2)	(3)	(4)	(5)	(6)	(7)
a025	0.25	HW criteria	1	20	413	158
a025qc15	0.25	1.50	1	14	283	105
a025qc17	0.25	1.70	1	12	207	80
a050	0.50	HW criteria	1	13	468	160
a025	0.25	HW criteria	3	42	462	198

Notes. (1) model name. (2) α value. (3) CE criteria for binaries with giant stars at the first mass transfer phase. (4) WD interior temperature (5)-(7) nova rates at 10 Gyr.

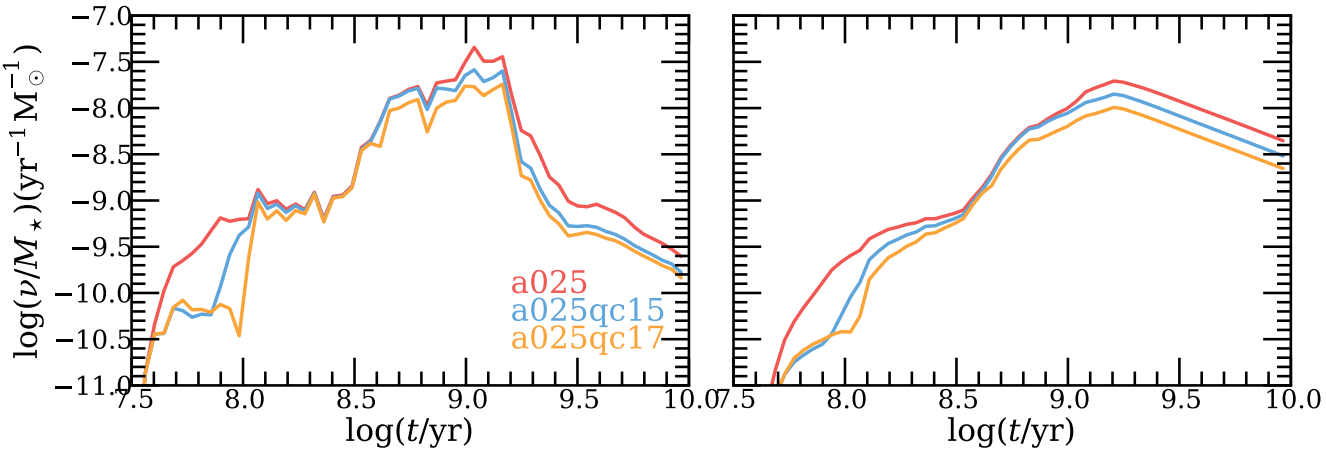

Figure 1. Evolution of mass-specific nova rates for elliptical-like galaxies (left panel) and spiral-like galaxies (right panel) in different models (see table 1). The red, blue, orange colours are for a025, a025qc15, a025qc17 model, respectively.

3.2 Current nova population

Since the properties of novae are mainly determined by the WD mass, we show the WD mass spectra of the "current" (10 Gyr) nova population in Fig. 3. The WD mass peaks around $0.5 - 0.6\,M_\odot$ in elliptical-like galaxies and $1.30 - 1.40\,M_\odot$ in spiral-like galaxies. This is expected; in elliptical-like galaxies, WD binaries with massive WDs evolve faster and the number of massive WDs decreases. Therefore, the typical WD mass of novae at 10 Gyr is small. The cut off at the low mass side is simply due to the fact that we ignore He WDs in our calculation. In spiral-like galaxies, there are young stellar populations with massive WDs. Most of these WDs have initially small mass and have increased their mass during the thermal timescale mass transfer (see Fig. 2 of Chen et al. (2014)). From Yaron et al. (2005), we know that the ignition mass of novae for massive WDs can be smaller by $2-3$ orders of magnitude, compared with low mass WDs. Therefore, massive WDs can have relatively more frequent nova outbursts. In M31-like galaxies, there are two peaks in the WD spectra. The peak around low WD mass is simply due to the large number of WD binary systems with low mass WDs. The peak around massive WD mass is due to massive WDs having more frequent nova outbursts.

In Fig. 4, we show the mass loss time ($t_{\rm ml}$) distribution of novae for different kinds of galaxies and compare the result of M31-like galaxies with the observational data of M31. With respect to the observational data, identical to the above description of the observed nova rate in M31, we combine the nova data of Arp (1956) and Darnley et al. (2006). With the results of Yaron et al. (2005), we can get two timescales for each novae - the decay time of bolometric luminosity by 3 mag $t_{3,\rm bol}$ and the duration of mass loss phase $t_{\rm ml}$. It is found that $t_{\rm ml}$ is much closer to the observed t_3 than $t_{3,\rm bol}$ (Prialnik & Kovetz 1995; Yaron et al. 2005). The following formula is used to compute the values of $t_{\rm ml}$ for observed novae (Bode & Evans 2008).

$$t_2 = \begin{cases} t_{\rm ml}/2.1 & t_{\rm ml} < 50 \text{ days} \\ t_{\rm ml}/1.75 & t_{\rm ml} \geq 50 \text{ days} \end{cases}$$

One point worth noting is that using a higher and fixed critical mass ratio in the CE criteria does not result in an unrealistic nova population. In elliptical-like galaxies, novae have a typical mass loss time around hundreds of days. The mass loss time of novae in spiral-like galaxies peaks around several tens of days. In M31-like galaxies, the mass loss time of novae ranges from tens of days to hundreds of days. Compared with the observational data of M31, there are too many novae predicted with $t_{\rm ml} < 10$ days and $t_{\rm ml} > 300$ days. Although Soraisam & Gilfanov (2015) and Soraisam et al.

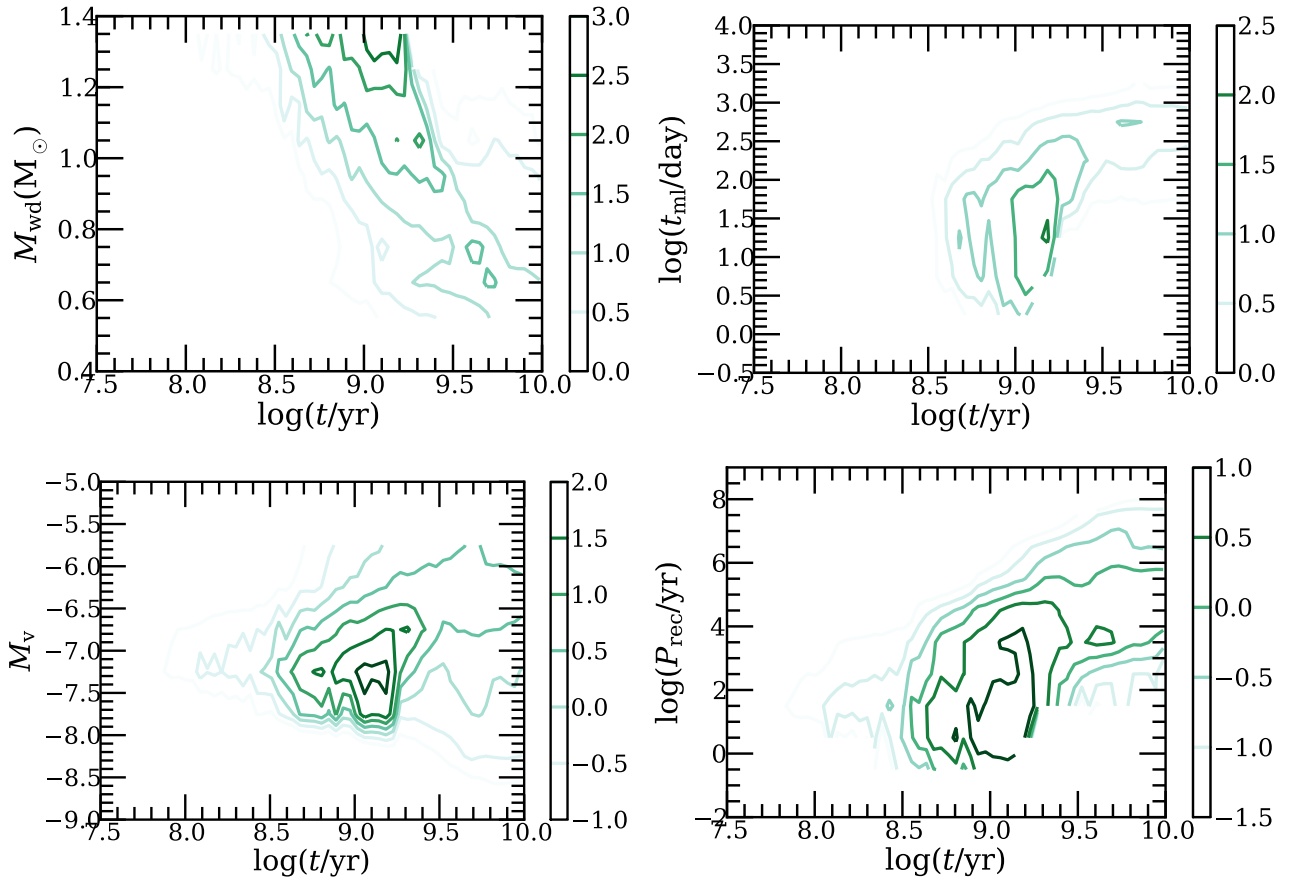

Figure 2. Isodensity contours for nova properties at different stellar ages for elliptical-like galaxies in a025 model. The values of different contours are for $(\partial^2 N/\partial {\rm log}t\partial M_{\rm WD})/M_\star$(upper left), $(\partial^2 N/\partial {\rm log}t\partial {\rm log}t_{\rm tml})/M_\star$ (upper right), $(\partial^2 N/\partial {\rm log}t\partial M_{\rm v})/M_\star$ (lower left), $(\partial^2 N/\partial {\rm log}t\partial {\rm log}P_{\rm rec})/M_\star$ (lower right) in logarithm. N is the number of nova events and $M_\star$ is the stellar mass of the galaxy.

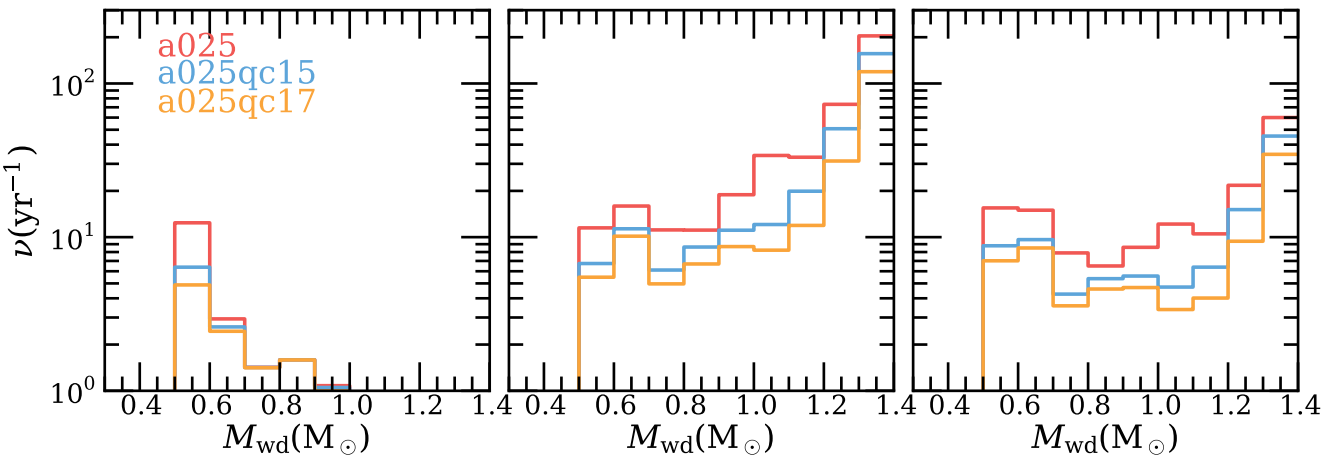

Figure 3. Distribution of nova rate as a function of WD mass for current nova population of elliptical-like galaxies (left panel), spiral-like galaxies (middle panel) and M31-like galaxies (right panel) in different models (see table 1). The red, blue, orange colours are for a025, a025qc15, a025qc17 model, respectively.

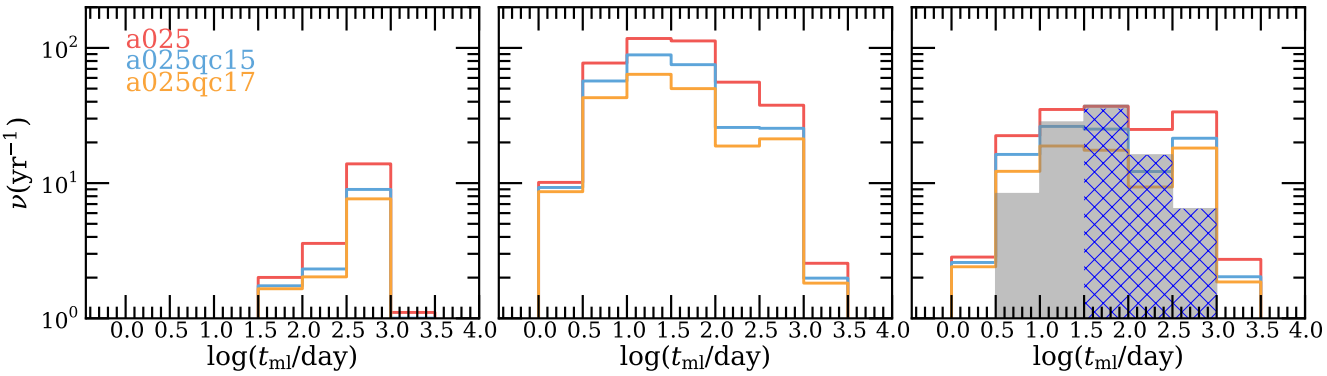

Figure 4. Mass loss time distribution of current nova population of elliptical-like galaxies (left panel), spiral-like galaxies (middle panel) and M31-like galaxies (right panel) in different models (see table 1). The red, blue, orange colours are for a025, a025qc15, a025qc17 model, respectively. The gray histogram shows the combined observational nova data from Arp (1956) and Darnley et al. (2006) taking the incompleteness into consideration (Soraisam & Gilfanov 2015; Soraisam et al. 2016). The shaded histogram shows the observational nova data of Darnley's paper only.

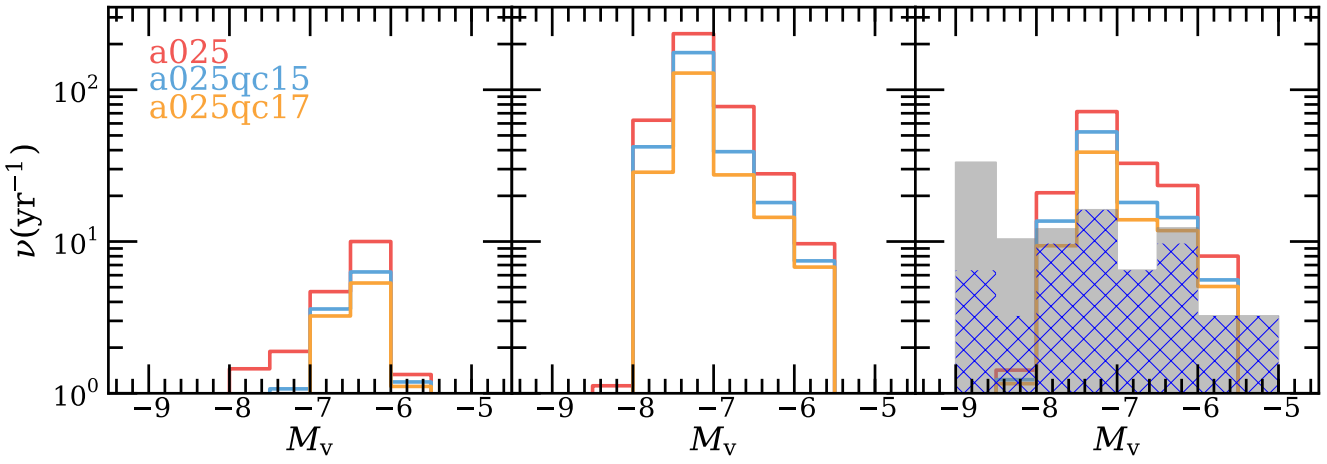

Figure 5. Distribution of V band maximum magnitude for current nova population of elliptical-like galaxies (left panel), spiral-like galaxies (middle panel) and M31-like galaxies (right line) in different models (see table 1). The red, blue, orange colours are for a025, a025qc15, a025qc17 model, respectively. The gray histogram shows the combined observational nova data from Arp (1956) and Darnley et al. (2006) taking the incompleteness into consideration (Soraisam & Gilfanov 2015; Soraisam et al. 2016). The shaded histogram shows the observational nova data from Darnley et al. (2006) only.

(2016) have corrected for the incompleteness of the short events, their correction was approximate and may not be accurate enough for the shortest novae. No incompleteness was applied for the longest events in our comparison. The novae with the shortest mass loss times are easily missed in observations, since observations are usually discontinuous. On the other hand, the novae with the longest mass loss times may be difficult to detect, because these novae are likely to be faint and the luminosity may not dramatically decline within the limited observational time.

Following Shafter et al. (2009), we assume that the colour of novae at maximum luminosity is the same as the colour of an A5V star ($T_{\mathrm{eff}} \sim 8200$ K). Then we can get the V band magnitude of novae for any given maximum bolometric luminosity with the data compiled by Johnson (1966). In Fig. 5, we show the distribution of V-band magnitude for novae at maximum luminosity. The novae are dominated by those with M_{v} from about -7.0 to about -6.0 in elliptical-like galaxies while absolute V-band magnitude peaks around about -8.0 to -6.5 in spiral-like and M31-like galaxies. Arp (1956) found that the maximum photographic magnitude of novae in M31 has a bimodal distribution. However, in M31-like galaxies, we do not find a bimodal distribution in the theoretical and observational results. The observational data of M31 is shown in the right panel of Fig. 5, which is based on the results of Arp (1956) and Darnley et al. (2006). In the Arp's survey, the photographic magnitudes were given. We correct them for the foreground extinction with $A_{\mathrm{pg}} = 0.25$ (Shafter et al. 2009). Then we convert the photographic magnitude to V-band magnitude using colours $(B - m_{\mathrm{pg}}) = 0.17$ (Arp 1956; Capaccioli et al. 1989) and $(B - V) = 0.15$ (Shafter et al. 2009). For novae from Darn-

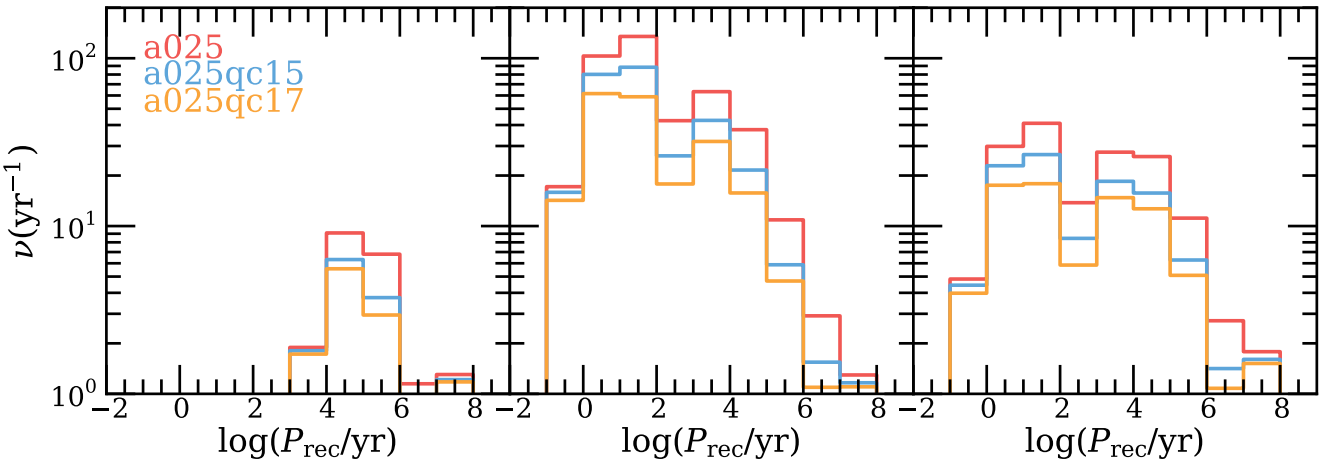

Figure 6. Distribution of recurrence period for current nova population of elliptical-like galaxies (left panel), spiral-like galaxies (middle panel) and M31-like galaxies (right panel) in different models (see table 1). The red, blue, orange colours are for a025, a025qc15, a025qc17 model, respectively.

ley et al. (2006), we convert the observed magnitude to V-band magnitude using colour $(V-R)=0.16$ (Shafter et al. 2009). Compared with the observational data, we underestimate the number of very bright novae. The possible reasons for this discrepancy are as follows. First, we did not include low temperature WDs ($T_{\rm c}<1.0\times10^7$ K) in our calculation. With the same code used by Yaron et al. (2005), Shara et al. (2010) (see also Schwartzman et al. (1994)) found that some very luminous novae can be explained by low temperature WDs with low accretion rates. Additionally, as Prialnik & Kovetz (1995) discussed, the error in the maximum luminosity in their simulations can be as large as −0.75 magnitude. Finally, in our calculation of $M_{\rm v}$, we assume that the spectra of all novae at maximum are similar to normal A5V main sequence stars. However, previous studies (e.g. Bode & Evans 2008) found that the spectra of novae at maximum resemble the spectra of stars with spectral type in the range B5 to F5. Recently, based on high quality photometric spectra of novae, Munari (2014) found that the spectra of some novae deviate from A5 main sequence stars (see his Fig. 4). For example, the colour (B-V) ranges from around 0.20 to 3.40, while (B-V) = 0.15 for A5V main sequence stars. This evidence suggests that adopting a unique spectral type may not be an accurate assumption. This will influence the colour and bolometric correction used in the above conversion.

In Fig. 6, we show the distribution of recurrence periods for novae in different galaxy types given different models. The novae in elliptical-like galaxies have relatively long recurrence periods, while the novae in spiral-like galaxies have predominantly shorter recurrence periods. In M31-like galaxies, there are two peaks, which correspond to the two peaks of the WD mass distribution in Fig. 3. The peak around massive WD produces the peak around short recurrence periods; most of these WDs have accumulated additional mass during a prior thermal timescale mass transfer phase. These massive WDs have more frequent outbursts and are also short lived (see Fig. 2). The peak around small WD masses corresponds to the peak around long recurrence periods. In spiral-like galaxies, there is a large number of WD binaries with small WD mass. But these small WDs have less frequent outbursts. Given the short observational time in reality, less novae, particularly recurrent novae, will be detected in elliptical galaxies. If we take the novae with recurrence period $P_{\rm rec}<100$ yr as recurrent novae, there will be no recurrent novae in elliptical-like galaxies. In spiral-like galaxies, the fraction of recurrent novae is around $\sim 60\%-65\%$. In M31-like galaxies, the fraction of recurrent novae is $\sim 45\%-50\%$. Shafter et al. (2015) performed a thorough astrometric study of novae in M31 and did a Monte Carlo analysis of the detection effficiency of recurrent novae. They suggested that as many as one in three M31 novae may be recurrent novae with $P_{\rm rec}<100\,$yr. Our result is not inconsistent with their results.

4 DISCUSSION

4.1 Influence of α values

As we discussed in section 2, the appropriate value(s) of α suffers from considerable uncertainty. Therefore, we computed a model with $\alpha=0.5$ (a050 model) and found no dramatic difference between the results of this model and a025 model, which is similar to what we found in Chen et al. (2014). Here we only show the distribution of recurrence period for comparison in Fig. 7. The influence of α values on the evolution of the binary population is rather complicated. Qualitatively it is clear that for larger α values more binaries will survive from the first CE phase and typical binary separations of survivors will become larger. For larger binary separations, in more binary systems the mass loss of non-degenerate donors upon ROLF will be unstable and a fraction of population underlaying novae will be lost. As well, in remaining systems accretion rates will be higher and WD may spend more time as stably nuclear burning objects and less as nova progenitors (less mass will be left for unstable burning). But the last effect may be offset by the increased WD mass and WDs with higher accretion rates have lower ignition mass. As a result,the total nova rates remain com-

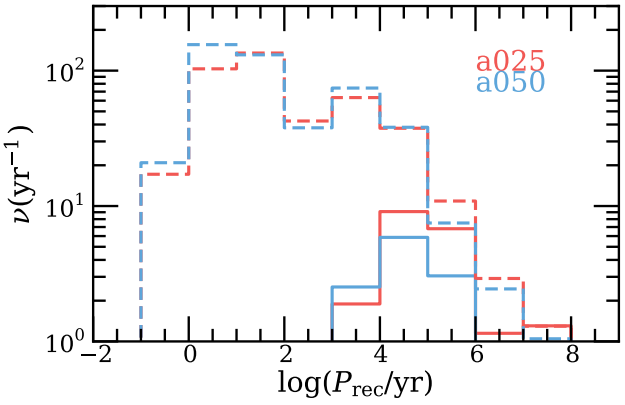

Figure 7. Comparison of recurrence period distribution of current nova population for elliptical-like (solid line) and spiral-like galaxies (dashed line) in a025 model (red line) and a050 model (blue line).

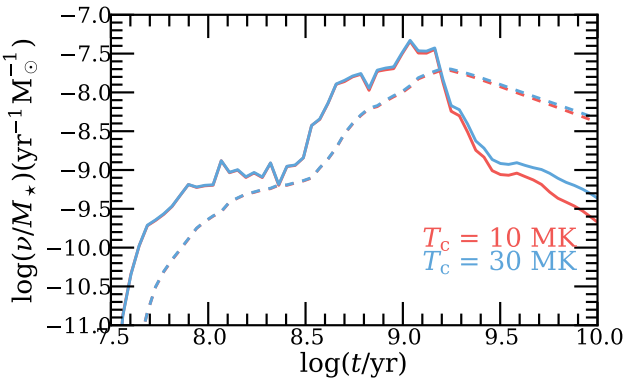

Figure 8. Mass-normalized nova rates as a function of stellar age for elliptical-like galaxies (solid line) and spiral-like galaxies (dashed line) in a025 model assuming WD temperatures $T_{\mathrm{c}} = 1 \times 10^7$ K (red colour), $T_{\mathrm{c}} = 3 \times 10^7$ K (blue colour).

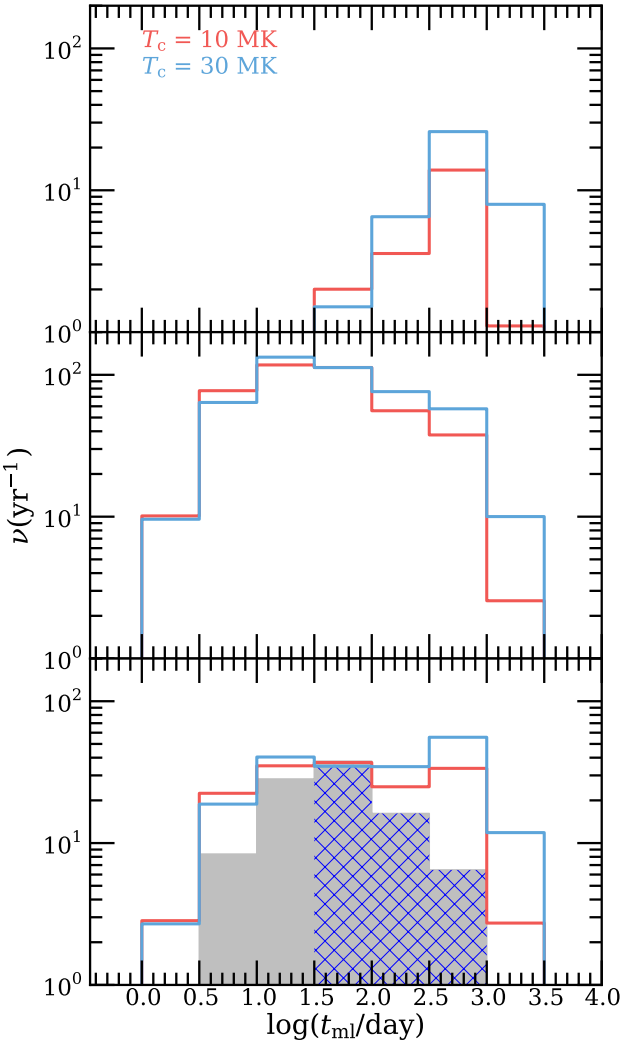

Figure 9. Mass loss time distribution of current nova population for elliptical-like galaxies (upper panel), spiral-like galaxies (middle panel) and M31-like galaxies (lower panel) in a025 model assuming WD temperatures $T_{\mathrm{c}} = 1 \times 10^7$ K (red colour), $T_{\mathrm{c}} = 3 \times 10^7$ K (blue colour). The gray histogram shows the observational nova data from Arp (1956) and Darnley et al. (2006) taking the incompleteness into consideration (Soraisam & Gilfanov 2015; Soraisam et al. 2016). The shaded histogram shows the observational nova data of Darnley et al. (2006) only.

parable. A more thorough study of this issue is beyond the scope of the present paper.

4.2 Influence of WD interior temperatures

In the above nova calculation, we assume that the interior temperatures of WDs are constant, i.e. $T_{\mathrm{c}} = 1.0 \times 10^7$ K. In order to understand the influence of WD temperature on our results, we computed a model with $T_{\mathrm{c}} = 3.0 \times 10^7$ K. The other assumptions of this model are the same as in a025 model.

From Fig. 8, we see that there is no dramatic difference among models with different WD temperatures and nova rates are only slightly higher for WDs with higher temperatures (see also table 1). This can be understood since the ignition mass of novae is lower for WDs with higher temperature (Yaron et al. 2005). In elliptical-like galaxies, the difference becomes larger at old ages. This is due to the fact that the difference in ignition mass at different temperatures is larger for low WD masses than for massive WD (Yaron et al. 2005).

In Fig. 9, we show the distribution of mass loss time at 10 Gyr in different types of galaxies for a025 model assuming different WD temperatures. Compared with model with WD temperature $T_{\mathrm{c}} = 1.0 \times 10^7$ K, there is an enhancement of novae with long mass loss times ($t_{\mathrm{ml}} > 100$ days) for all galaxies types in the model with a higher WD temperature. In Fig. 10, we show the distribution of recurrence period of novae. There is an enhancement of novae with long recurrence period for the model with a high WD temperature. The trend seen in Figs. 9 and 10 is explained by the fact that, at $\dot{M}_{\mathrm{acc}} \leq 10^{-8}\,M_\odot\,\mathrm{yr}^{-1}$ at which most of novae oc-

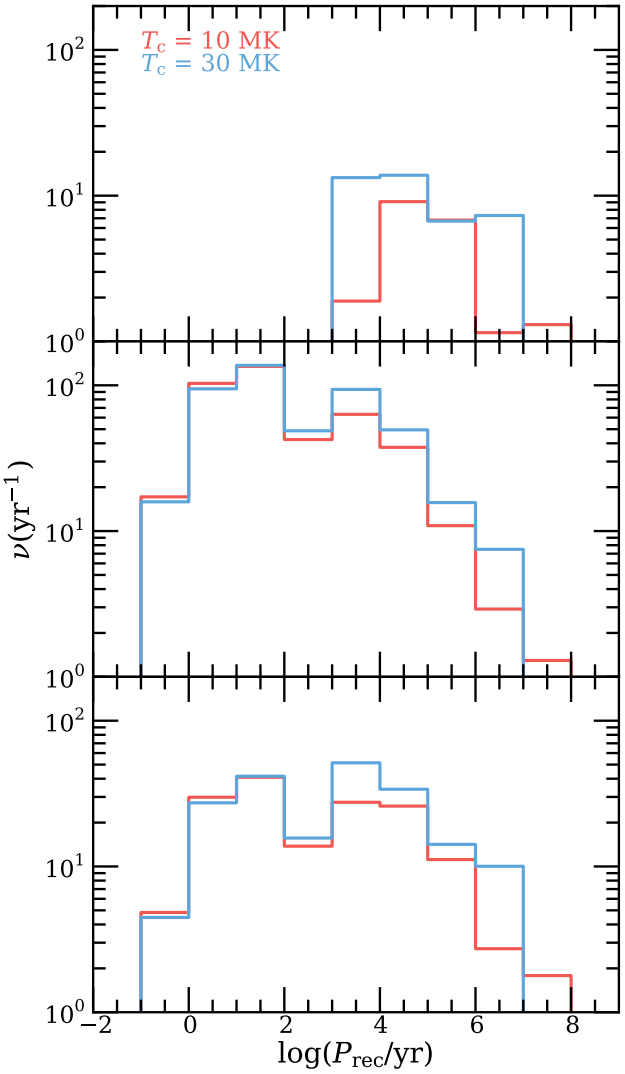

Figure 10. Recurrence period distribution of current nova population for elliptical-like galaxies (upper panel), spiral-like galaxies (middle panel) and M31-like galaxies (lower panel) in a025 model assuming WD temperatures $T_c = 1 \times 10^7$ K (red colour), $T_c = 3 \times 10^7$ K (blue colour).

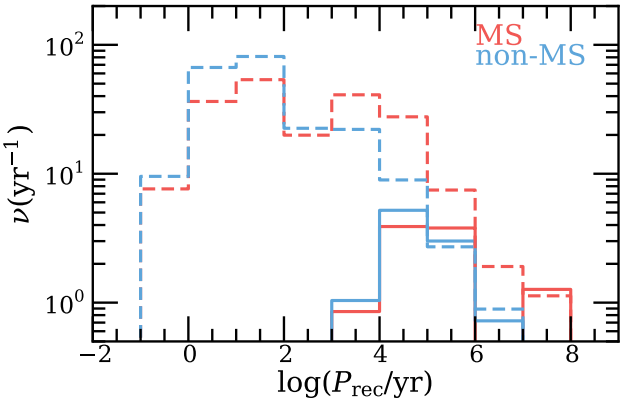

Figure 11. Distribution of recurrence period for current nova population with different types of donors in elliptical-like (solid line) and spiral-like galaxies (dashed line). The red and blue lines shows the novae with MS donors and non-MS donors (i.e. HGs and RGs), respectively. The donor type is defined according to the donor type at the onset of mass transfer.

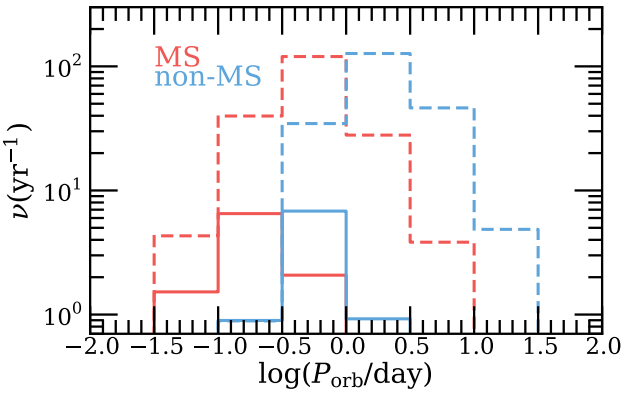

Figure 12. Distribution of orbital periods for current nova population with different types of donor in elliptical-like (solid line) and spiral-like galaxies (dashed line). The red and blue lines shows the novae with MS donors and non-MS donors (i.e. HGs and RGs), respectively. The donor type is defined according to the donor type at the onset of mass transfer.

cur, $P_{\rm rec}$ drops with increase of T_c, while $t_{\rm ml}$ increases with increase of T_c (Yaron et al. 2005).

4.3 Influence of metallicity

Saglia et al. (2010) found that in the inner few arcsecs of the bulge of M31, the metallicity is $\sim 3\,Z_\odot$. Except for this region, the metallicity is solar. In addition, the metallicity of the disc is less than solar. In our computation, we assume that the metallicity of the stellar population is solar. The influence of metallicity on our results is rather complicated. First, it will influence the binary evolution. For example, Meng et al. (2008) found that, for $Z \geq 2Z_\odot$, the final WD mass will increase as metallicity increases, while for metallicity $Z < 2Z_\odot$, it will decrease as metallicity increases. Additionally, Piersanti et al. (2000) computed the evolution of accreting WDs for H-rich material with different metallicities and they found that the accretion rate for stably burning WD will be lower for lower metallicity and the width of the stably burning regime will be reduced. On the other hand, metallicity will influence the nova properties. For example, Starrfield et al. (2000) have studied the effects of metallicity on nova outburst and found that the ignition mass is higher for lower metallicity. Although metallicity is important in our calculation, it is difficult for us to quantitatively assess its influence on our results, and further studies are needed in this regard.

4.4 Novae with donors at differing evolutionary states

We classify novae according to the donor type at the onset of mass transfer. In Fig. 11, we show the recurrence period

distribution of the "current" nova population with different donor types in elliptical-like galaxies and spiral-like galaxies. The contribution to the total nova rate from WD binaries with non-MS donors is comparable to that of WD binaries with MS donors. This conclusion is also true for our model of a M31-like galaxy. In Fig. 12, we show the orbital period distribution of the current nova population in elliptical-like and spiral-like galaxies. It is found that the secondaries of those novae with non-MS donors are mainly located in the hydrogen-shell burning stage. Those WD binaries with evolved secondaries have relatively higher mass transfer rates. In addition, the WD will accumulate mass during the thermal timescale mass transfer. For higher mass transfer rates and large WD masses, the ignition mass will be smaller. Therefore, there will be more frequent outbursts for these binaries.

Williams et al. (2014) found 11 nova progenitor systems with evolved secondaries in a survey with 38 confirmed nova progenitor systems. This leads to a fraction of $\sim 30\%$ of the nova progenitor systems which harbour evolved secondaries. Given the nova progenitor systems with evolved secondaries have relatively higher mass transfer rates compared with nova progenitor systems with MS donors, nova progenitor systems with evolved secondaries should have more frequent outbursts. Therefore, the contribution of novae with evolved donors to the total nova rate should be larger than the fraction of corresponding binary systems, 30%. Recently, Williams et al. (2016) conducted a more accurate statistical analysis of their preceding results and came to the conclusion that $\sim 30^{+13}_{-10}\%$ of nova eruptions in M31 Galaxy are RG-novae.

4.5 Correlation between mass-specific nova rate and morphological type of galaxy

Observations give contradicting results regarding the dependence of the mass-specific nova rate on the Hubble type of the galaxy. Some observational studies (e.g. Ciardullo et al. 1990; Shafter et al. 2000; Ferrarese et al. 2003; Williams & Shafter 2004) claimed that there is no strong dependence of mass-specific nova rate on the Hubble types of galaxies: the majority of galaxies have around $2 \pm 1 \times 10^{-10} {L_{\odot,K}}^{-1}\,\mathrm{yr}^{-1}$. However, there are several galaxies which may have a higher mass-specific nova rate, e.g. the SMC, LMC, M33 and others(Della Valle et al. 1994; Della Valle 2002; Neill & Shara 2005; Alis & Saygac 2014; Shara et al. 2016). The mass-specific nova rate of elliptical-like galaxies at 10 Gyr in our calculation is around $(1-2) \times 10^{-10}\,{\mathrm{M}_\odot}^{-1}\,\mathrm{yr}^{-1}$. This is consistent with Williams & Shafter (2004), since the total stellar mass-to-light ratio $M_\star/L_\mathrm{K} \sim 1.0$, slightly depending on the colour of the galaxy (Bell & de Jong 2001). However, for spiral-like galaxies, we obtained a mass-specific nova rate 10-20 times larger. It would seem then that our results are inconsistent with measurements of Williams & Shafter (2004). However, one crucial point to understand this discrepancy is the incompleteness of nova surveys. For example, the nova rate of M31 in the analysis of Williams & Shafter (2004) is significantly lower than the nova rates of Darnley et al. (2006). As we discussed above, a more reliable value should be $\approx 97\,\mathrm{yr}^{-1}$, giving a luminosity-specific nova rate $\sim 7.0 \times 10^{-10}\,{L_{\odot,K}}^{-1}\,\mathrm{yr}^{-1}$, which is a factor of $3-4$ larger than the value in Williams & Shafter (2004). In our model for M31, we find a mass-specific nova rate of $\approx (7-14) \times 10^{-10}\,{\mathrm{M}_\odot}^{-1}\,\mathrm{yr}^{-1}$, which is consistent with the above number. In our model of spiral-like galaxies, we assume the SFR to be constant, which is almost certainly oversimplified in the general case. As shown in Figs. 1 and 2, if there was an initial spike of SFR, certain fraction of total mass of "realistic" spirals sits in old population which does not contribute much to the current nova rate. This will lead to a smaller value of luminosity-specific nova rate (cf. table 1).

4.6 Novae with short recurrence periods

In M31-like galaxies, the predicted rate of novae with recurrence period $P_\mathrm{rec} < 1\,\mathrm{yr}$ is around $4\,\mathrm{yr}^{-1}$ (see Fig. 6). The typical WD mass of these novae is $1.30 - 1.40\,\mathrm{M}_\odot$ and their typical accretion rate is $10^{-7} - 10^{-6}\,\mathrm{M}_\odot\,\mathrm{yr}^{-1}$. Recently, Tang et al. (2014) discovered a nova with recurrence period of around 1 yr, and Henze et al. (2015) found the recurrence period of this nova is more likely to be 6 months. Based on the recurrence period and the X-ray emission, Tang et al. (2014) constrained the WD mass of the nova to be $> 1.30\,\mathrm{M}_\odot$ and its accretion rate to be $> 1.7 \times 10^{-7}\,\mathrm{M}_\odot\,\mathrm{yr}^{-1}$. Presently, this is the only nova with a recurrence period less than 1 yr detected in M31 giving a nova rate $\sim 2\,\mathrm{yr}^{-1}$. We predict a rate of around $4\,\mathrm{yr}^{-1}$. Given the uncertainties of observations and simulations, our results for short recurrence periods are consistent with observations.

4.7 Novae with ONe WDs

In our calculation, we do not distinguish ONe WDs from CO WDs. Evidently, some massive WDs should be ONe WDs. José & Hernanz (1998) found that ONe WDs have higher ignition masses (about a factor of 2), compared with CO WDs. This is due to the lower ^{12}C abundance in the envelope which will reduce the reaction rate of the CNO cycle and less energy will be released at the same temperature. Therefore, the ONe WDs should have longer recurrence periods. However, the difference of t_ml and M_V between ONe WD and CO WD with same mass has not been investigated. Assuming that the ignition mass of novae for ONe WD is the same as for CO WD, we compute the nova rate of ONe WDs based on the WD type identification in BSE code. We find that, for the current nova population in elliptical-like and spiral-like galaxies, the contribution of ONe WDs to the total nova rate is rather small (less than 10%).

4.8 Novae in Globular Clusters

Motivated by observations that the mass-specific number of low mass X-ray binaries is enhanced in globular clusters (GCs) (e.g. Clark 1975), it is also expected that a significant population of WD binaries could be formed through dynamical process in GCs (e.g. Bailyn 1991). Observations from the Chandra X-Ray Observatory and the Hubble Space Telescope have revealed dozens of cataclysmic variables in GCs (e.g. Grindlay et al. 2001; Heinke et al. 2005; Pooley et al. 2002). Consequently, we will expect the nova rate to be enhanced in GCs. So far, there are five novae found in GCs: one in M80 (Dieball et al. 2010), one in a GC of M87 (Shara

et al. 2004), two in the GCs of M31 (Shafter & Quimby 2007; Henze et al. 2013), and one in a GC of M84 (Curtin et al. 2015). Based on the two novae discovered in the GCs of M31 (Henze et al. 2013), the estimated nova rate in the M31 GC system is $0.05\,\mathrm{yr}^{-1}\,\mathrm{GC}^{-1}$. Curtin et al. (2015) found two novae in the GCs of M87 and M84 and estimated that novae are likely enhanced by at least an order of magnitude in GCs compared with the field. This evidence indicates that dynamical interactions in GCs may be an important factor in the calculation of the nova rate in a galaxy. Obviously, in our calculation, we do not take GCs into consideration.

5 CONCLUSIONS

With a hybrid binary population synthesis method, we have modelled the nova population for a starburst (i.e. elliptical-like galaxies) and a constant SFR model (i.e. spiral-like galaxies). In addition, we have also provided a composite model as an analog of M31 (i.e. M31-like galaxies). We have computed the nova rates and the nova properties, such as their distributions of mass loss time, maximum magnitude, for different stellar populations. We compare these results with observational data of M31. Our main results are summarized as follows.

1) We computed the nova rates as a function of stellar age in elliptical-like and spiral-like galaxies (see Fig. 1). In elliptical-like galaxies, the mass normalized nova rate peaks around 1 Gyr and declines by ~ 2 orders of magnitude at 10 Gyr. In spiral-like galaxies, it peaks around 2 Gyr and declines by a factor of ~ 4 in spiral-like galaxies at 10 Gyr. The mass-specific nova rate for elliptical-like galaxies at 10 Gyr in our calculation is $\sim (1-2)\times10^{-10}\,\mathrm{M}_{\odot}{}^{-1}\,\mathrm{yr}^{-1}$, which is consistent with observations. However, the mass-specific nova rate for spiral-like galaxies at 10 Gyr is $\sim (20-40)\times10^{-10}\,\mathrm{M}_{\odot}{}^{-1}\,\mathrm{yr}^{-1}$, which is larger than seen in some observations. The mismatch may be due to both the incompleteness of past surveys and the assumption of a constant SFR in our model. Moreover, our predictions go in the direction suggested by several papers which found high luminosity-specific nova rates in late-type systems like LMC and M33 (e.g. Della Valle et al. 1994; Della Valle 2002; Alis & Saygac 2014).

2) The current nova population is dominated by novae with low mass WDs in elliptical-like galaxies and by novae with massive WDs in spiral-like galaxies.

3) In elliptical-like galaxies, the majority of current novae have long mass loss times, are relatively faint, and have long recurrence periods. In spiral-like galaxies, the majority of the current nova population have short mass loss times, are relatively bright, and have short recurrence periods.

4) Given the uncertainties in both our calculation and observations, the predicted nova rate and the distribution of nova mass loss times in our M31-like galaxy are in good agreement with observational data for M31. The observed distribution may be subject to incompleteness at $t_{\rm ml} < 10$ day and $t_{\rm ml} > 300$ day. In addition, it is possible that we underestimate the number of very bright novae in our calculations. This may be due to the lack of low temperature WDs or the assumption of a unique spectral type for novae at the maximum luminosity in our work.

ACKNOWLEDGEMENTS

We would like thank the referee for useful comments, which helped to improve the paper. HLC would like to thank Monika Soraisam and Hans Ritter for helpful discussion about the calculation of novae. We are grateful to the MESA council for the MESA instrument papers and website. HLC gratefully acknowledges support and hospitality from the MPG-CAS Joint Doctoral Promotion Program (DPP) and the Max Planck Institute for Astrophysics (MPA). Z. H. is partially supported by the National Natural Science Foundation of China (Grant No.11390374,11521303), Science and Technology Innovation Talent Programme of Yunnan Province (Grant No. 2013HA005) and the Chinese Academy of Sciences (Grant Nos. XDB09010202, KJZD-EW-M06-01). The work was partially supported by Basic Research Program P-7 of the Presidium of the Russian Academy of Sciences and RFBR grants No. 14-02-00604 and 15-02-04053. LRY gratefully acknowledges warm hospitality and support from MPA-Garching. MG acknowledges hospitality of the Kazan Federal University (KFU) and support by the Russian Government Program of Competitive Growth of KFU. HLC acknowledges the computing time granted by the Yunnan Observatories and provided on the facilities at the Yunnan Observatories Supercomputing Platform.

REFERENCES

Alis S., Saygac A. T., 2014, in Woudt P. A., Ribeiro V. A. R. M., eds, Astronomical Society of the Pacific Conference Series Vol. 490, Stellar Novae: Past and Future Decades. p. 95
Arp H. C., 1956, AJ, 61, 15
Bailyn C. D., 1991, in Janes K., ed., Astronomical Society of the Pacific Conference Series Vol. 13, The Formation and Evolution of Star Clusters. pp 307–323
Barmby P., et al., 2007, ApJ, 655, L61
Bell E. F., de Jong R. S., 2001, ApJ, 550, 212
Bode M. F., Evans A., 2008, Classical Novae
Capaccioli M., Della Valle M., Rosino L., D'Onofrio M., 1989, AJ, 97, 1622
Chen X., Han Z., 2008, MNRAS, 387, 1416
Chen H.-L., Woods T. E., Yungelson L. R., Gilfanov M., Han Z., 2014, MNRAS, 445, 1912
Chen H.-L., Woods T. E., Yungelson L. R., Gilfanov M., Han Z., 2015, MNRAS, 453, 3024
Ciardullo R., Ford H. C., Neill J. D., Jacoby G. H., Shafter A. W., 1987, ApJ, 318, 520
Ciardullo R., Tamblyn P., Jacoby G. H., Ford H. C., Williams R. E., 1990, AJ, 99, 1079
Clark G. W., 1975, ApJ, 199, L143
Coelho E. A., Shafter A. W., Misselt K. A., 2008, ApJ, 686, 1261
Curtin C., Shafter A. W., Pritchet C. J., Neill J. D., Kundu A., Maccarone T. J., 2015, ApJ, 811, 34
Darnley M. J., et al., 2006, MNRAS, 369, 257
Darnley M. J., et al., 2014, in Woudt P. A., Ribeiro V. A. R. M., eds, Astronomical Society of the Pacific Conference Series Vol. 490, Stell Novae: Past and Future Decades. p. 49 (arXiv:1303.2711)
Davis P. J., Kolb U., Willems B., 2010, MNRAS, 403, 179
Davis P. J., Kolb U., Knigge C., 2012, MNRAS, 419, 287
de Kool M., 1990, ApJ, 358, 189
Della Valle M., 2002, in Hernanz M., José J., eds, American Institute of Physics Conference Series Vol. 637, Classical Nova Explosions. pp 443–456 (arXiv:astro-ph/0210276), doi:10.1063/1.1518244

Della Valle M., Livio M., 1998, ApJ, 506, 818
Della Valle M., Bianchini A., Livio M., Orio M., 1992, A&A, 266, 232
Della Valle M., Rosino L., Bianchini A., Livio M., 1994, A&A, 287, 403
Dieball A., Long K. S., Knigge C., Thomson G. S., Zurek D. R., 2010, ApJ, 710, 332
Duerbeck H. W., 1990, in Cassatella A., Viotti R., eds, Lecture Notes in Physics, Berlin Springer Verlag Vol. 369, IAU Colloq. 122: Physics of Classical Novae. p. 34, doi:10.1007/3-540-53500-4_90
Ferrarese L., Côté P., Jordán A., 2003, ApJ, 599, 1302
Franck J. R., Shafter A. W., Hornoch K., Misselt K. A., 2012, ApJ, 760, 13
Gehrz R. D., Truran J. W., Williams R. E., Starrfield S., 1998, PASP, 110, 3
Giannone P., Weigert A., 1967, ZAp, 67, 41
Grindlay J. E., Heinke C., Edmonds P. D., Murray S. S., 2001, Science, 292, 2290
Hachisu I., Kato M., 2001, ApJ, 558, 323
Hachisu I., Kato M., Nomoto K., 1996, ApJ, 470, L97
Hachisu I., Kato M., Nomoto K., 1999, ApJ, 522, 487
Han Z., Podsiadlowski P., Maxted P. F. L., Marsh T. R., Ivanova N., 2002, MNRAS, 336, 449
Heinke C. O., Grindlay J. E., Edmonds P. D., Cohn H. N., Lugger P. M., Camilo F., Bogdanov S., Freire P. C., 2005, ApJ, 625, 796
Henze M., et al., 2013, A&A, 549, A120
Henze M., Darnley M. J., Kabashima F., Nishiyama K., Itagaki K., Gao X., 2015, A&A, 582, L8
Hernanz M., Jose J., Coc A., Isern J., 1996, ApJ, 465, L27
Hillman Y., Prialnik D., Kovetz A., Shara M. M., 2015, preprint, (arXiv:1508.03141)
Hjellming M. S., Webbink R. F., 1987, ApJ, 318, 794
Hurley J. R., Tout C. A., Pols O. R., 2002, MNRAS, 329, 897
Idan I., Shaviv N. J., Shaviv G., 2013, MNRAS, 433, 2884
Ivanova N., et al., 2013, A&A Rev., 21, 59
Izzo L., et al., 2015, ApJ, 808, L14
Johnson H. L., 1966, ARA&A, 4, 193
José J., Hernanz M., 1998, ApJ, 494, 680
Kato M., Hachisu I., 2004, ApJ, 613, L129
Kouwenhoven M. B. N., Brown A. G. A., Goodwin S. P., Portegies Zwart S. F., Kaper L., 2009, A&A, 493, 979
Kraft R. P., 1964, ApJ, 139, 457
Kraicheva Z. T., Popova E. I., Tutukov A. V., Yungelson L. R., 1979, Soviet Ast., 23, 290
Kraus A. L., Hillenbrand L. A., 2009, ApJ, 703, 1511
Kroupa P., 2001, MNRAS, 322, 231
Kudryashov A. D., Chugaĭ N. N., Tutukov A. V., 2000, Astronomy Reports, 44, 170
Livio M., Govarie A., Ritter H., 1991, A&A, 246, 84
Loveridge A. J., van der Sluys M. V., Kalogera V., 2011, ApJ, 743, 49
Matteucci F., Renda A., Pipino A., Della Valle M., 2003, A&A, 405, 23
Meng X., Chen X., Han Z., 2008, A&A, 487, 625
Mestel L., 1952a, MNRAS, 112, 583
Mestel L., 1952b, MNRAS, 112, 598
Munari U., 2014, in Woudt P. A., Ribeiro V. A. R. M., eds, Astronomical Society of the Pacific Conference Series Vol. 490, Stell Novae: Past and Future Decades. p. 183
Neill J. D., Shara M. M., 2005, AJ, 129, 1873
Nelemans G., Siess L., Repetto S., Toonen S., Phinney E. S., 2016, ApJ, 817, 69
Nelson L. A., MacCannell K. A., Dubeau E., 2004, ApJ, 602, 938
Olsen K. A. G., Blum R. D., Stephens A. W., Davidge T. J., Massey P., Strom S. E., Rigaut F., 2006, AJ, 132, 271
Paczynski B., Zytkow A. N., 1978, ApJ, 222, 604
Passy J.-C., Herwig F., Paxton B., 2012, ApJ, 760, 90
Patterson J., 1984, ApJS, 54, 443
Pavlovskii K., Ivanova N., 2015, MNRAS, 449, 4415
Paxton B., Bildsten L., Dotter A., Herwig F., Lesaffre P., Timmes F., 2011, ApJS, 192, 3
Paxton B., et al., 2013, ApJS, 208, 4
Piersanti L., Cassisi S., Iben Jr. I., Tornambé A., 2000, ApJ, 535, 932
Piersanti L., Tornambé A., Yungelson L. R., 2014, MNRAS, 445, 3239
Politano M., 1996, ApJ, 465, 338
Politano M., Livio M., Truran J. W., Webbink R. F., 1990, in Cassatella A., Viotti R., eds, Lecture Notes in Physics, Berlin Springer Verlag Vol. 369, IAU Colloq. 122: Physics of Classical Novae. p. 386, doi:10.1007/3-540-53500-4_150
Pooley D., et al., 2002, ApJ, 569, 405
Prialnik D., Kovetz A., 1995, ApJ, 445, 789
Prialnik D., Shara M. M., Shaviv G., 1978, A&A, 62, 339
Prialnik D., Shara M. M., Shaviv G., 1979, A&A, 72, 192
Ricker P. M., Taam R. E., 2012, ApJ, 746, 74
Robertson B., Yoshida N., Springel V., Hernquist L., 2004, ApJ, 606, 32
Rosino L., 1964, Annales d'Astrophysique, 27, 498
Rosino L., 1973, A&AS, 9, 347
Rosino L., Capaccioli M., D'Onofrio M., Della Valle M., 1989, AJ, 97, 83
Saglia R. P., et al., 2010, A&A, 509, A61
Sana H., et al., 2012, Science, 337, 444
Schreiber M. R., Zorotovic M., Wijnen T. P. G., 2016, MNRAS, 455, L16
Schwartzman E., Kovetz A., Prialnik D., 1994, MNRAS, 269, 323
Shafter A. W., Irby B. K., 2001, ApJ, 563, 749
Shafter A. W., Quimby R. M., 2007, ApJ, 671, L121
Shafter A. W., Ciardullo R., Pritchet C. J., 2000, ApJ, 530, 193
Shafter A. W., Rau A., Quimby R. M., Kasliwal M. M., Bode M. F., Darnley M. J., Misselt K. A., 2009, ApJ, 690, 1148
Shafter A. W., et al., 2015, ApJS, 216, 34
Shara M. M., Zurek D. R., Baltz E. A., Lauer T. R., Silk J., 2004, ApJ, 605, L117
Shara M. M., Yaron O., Prialnik D., Kovetz A., Zurek D., 2010, ApJ, 725, 831
Shara M. M., Doyle T., Lauer T. R., Zurek D., Neill J. D., Madrid J. P., Welch D. L., Baltz E. A., 2016, preprint, (arXiv:1602.00758)
Sion E. M., Acierno M. J., Tomczyk S., 1979, ApJ, 230, 832
Soraisam M. D., Gilfanov M., 2015, A&A, 583, A140
Soraisam M. D., Gilfanov M., Wolf W. M., Bildsten L., 2016, MNRAS, 455, 668
Starrfield S., Truran J. W., Sparks W. M., Kutter G. S., 1972, ApJ, 176, 169
Starrfield S., Truran J. W., Sparks W. M., 1978, ApJ, 226, 186
Starrfield S., Sparks W. M., Shaviv G., 1988, ApJ, 325, L35
Starrfield S., Schwarz G., Truran J. W., Sparks W. M., 2000, in Holt S. S., Zhang W. W., eds, American Institute of Physics Conference Series Vol. 522, American Institute of Physics Conference Series. pp 379–382, doi:10.1063/1.1291739
Tajitsu A., Sadakane K., Naito H., Arai A., Aoki W., 2015, Nature, 518, 381
Tajitsu A., Sadakane K., Naito H., Arai A., Kawakita H., Aoki W., 2016, preprint, (arXiv:1601.05168)
Tang S., et al., 2014, ApJ, 786, 61
Townsley D. M., Bildsten L., 2004, ApJ, 600, 390
Truran J. W., Livio M., 1986, ApJ, 308, 721
Tutukov A. V., Ergma E. V., 1979, Soviet Astronomy Letters, 5, 284
Tutukov A. V., Yungel'Son L. R., 1972, Astrophysics, 8, 227
van Haaften L. M., Nelemans G., Voss R., Toonen S., Portegies Zwart S. F., Yungelson L. R., van der Sluys M. V., 2013, A&A,

552, A69
Webbink R. F., 1984, ApJ, 277, 355
Webbink R. F., 1988, The Formation and Evolution of Symbiotic Stars. p. 311
Williams S. J., Shafter A. W., 2004, ApJ, 612, 867
Williams S. C., Darnley M. J., Bode M. F., Keen A., Shafter A. W., 2014, ApJS, 213, 10
Williams S. C., Darnley M. J., Bode M. F., Shafter A. W., 2016, ApJ, 817, 143
Wolf W. M., Bildsten L., Brooks J., Paxton B., 2013, ApJ, 777, 136
Woods T. E., Ivanova N., 2011, ApJ, 739, L48
Yaron O., Prialnik D., Shara M. M., Kovetz A., 2005, ApJ, 623, 398
Yungelson L., Livio M., Truran J. W., Tutukov A., Fedorova A., 1996, ApJ, 466, 890
Yungelson L., Livio M., Tutukov A., 1997, ApJ, 481, 127
Zorotovic M., Schreiber M. R., Gänsicke B. T., Nebot Gómez-Morán A., 2010, A&A, 520, A86